Hydrochemical characteristics and microbial community evolution of Pinglu river affected by regional abandoned coal mine drainage, Guizhou province, China

Di Chen (xinmaichen919@163.com)
China university of mining and technology
Yun Zhang
China University of Mining and Technology School of Environment Science and Spatial Informatics
Qiyan Feng
China University of Mining and Technology School of Environment Science and Spatial Informatics

Research Article

Keywords: Abandoned coal mine, Acid mine drainage (AMD), Hydrochemical characteristics, Microbial community, Ca/Mg ratio, Bugbase phenotype prediction

Posted Date: April 7th, 2022

DOI: https://doi.org/10.21203/rs.3.rs-1409920/v1

Version of Record: A version of this preprint was published at Environmental Science and Pollution Research on May 8th, 2023. See the published version at https://doi.org/10.1007/s11356-023-27403-5.

Abstract

Acid mine drainage (AMD) from abandoned coal mines has become the main source of recharge for Pinglu River. The revelation of the hydrochemical characteristics of regional AMD contamination and the evolution of river microbial communities can contribute to the source management and ecological remediation of AMD pollution. In this study, we collected twelve abandoned coal mine drainage (group M), eight polluted river water samples (group R) and five river sediment samples for comprehensive analysis. Results indicated that SO_4-Ca·Mg was the main hydrochemical type of group M samples, and the Ca/Mg ratio of drainage was significantly negatively correlated with SO_4^{2-} (R^2=0.612, p<0.05). The confluence of AMD resulted in a gradual change of river hydrochemical type from SO_4·HCO_3-Ca·Mg to SO_4-Ca·Mg, accompanied by a simultaneous decrease in sediment microbial community diversity. In addition, significant differences in microbial community composition and diversity were observed between the upstream and downstream sediment of Pinglu river, and these differences were mainly attributed to pH, TOC and TP. Results of BugBase phenotype prediction demonstrated that the relative abundance of anaerobic microorganisms in river sediment gradually decreased from upstream to downstream (from 24.77 to 12.46%), which was mainly contributed by genera such as *Geobacter, Citrifermentans, Luteitalea* and *Vicinamibacter*.

Introduction

Coal occupies an important position in China's energy system, and the long-term high-intensity resource development has led to the depletion and decline of coal resources in several mining areas in China (Yuan 2019). Therefore, the Chinese government has issued and implemented a number of policies to consolidate the coal resources and close down the coal mines with outdated capacity. By the end of 2020, the total number of coal mines in China has been reduced from a maximum of more than 80,000 at the peak (Feng and Zhou 2016) to about 4,700. Approximately 95% of China's coal mines were underground mines. Groundwater will rebound into underground mines after the abandon of coal mines, making the underground mining area a potential source of pollution as a site for a variety of physical, chemical and biological reactions to occur (Chen et al. 2021a). Compared to production mines, water pollution from abandoned coal mines requires more attention. Wastewater in abandoned pits can cause cascading pollution of groundwater through channels such as fissures in mining areas, rock faults and closed poor boreholes (Feng and Zhou 2016), which significantly increases the difficulty and the cost of groundwater pollution management, in addition, such pollution cannot be controlled at source by effective measures. Moreover, due to the ineffectual management of abandoned coal mines, a considerable amount of wastewater from small abandoned coal mines without responsible entities will be discharged directly without treatment, causing serious surface environmental pollution problems.

Among all the types of coal mine water pollution, acid mine drainage (AMD) has the most prominent risk of contamination, which tends to have pH values between 2 and 4 and is prone to leaching of iron and manganese, as well as heavy metal such as lead, arsenic, chromium, and copper (Akcil and Koldas 2005). AMD in coal mines is widely recognized to occur when pyrite in coal seams and rocks in contact with air and water during high sulfur mining and is catalyzed by microorganisms (Acharya and Kharel 2020). However, AMD can still be generated after the abandon of coal mines and can even continue to discharge for decades. AMD from abandoned coal mines has posed a serious threat to the safety of regional surface water and groundwater systems. For example, the Hongshan and Zhaili coal mines in Zibo, Shandong Province of China, which have been closed for more than 20 years, still produce acid mine water, resulting in the contamination of about 50 km^2 of groundwater in the area (Zhang et al. 2015). AMD generated from the underground abandoned coal mines will continue to undergo a series of complex biogeochemical processes with the surrounding rocks and minerals during the migration with groundwater, which in

turn affects the ion types, contents and hydrochemical types of AMD. The study of the water hydrochemical characteristics of abandoned coal mine drainage can help to analyze the generation and transformation of AMD from the basic source, and lay the foundation for the pollution control and ecological remediation of AMD. In addition, AMD discharged into the surface environment can change the structure of ecosystems by altering the physicochemical properties of the surrounding environment and the composition structure of the microbial community (Sun et al. 2016a).

The coal seam in the Kaili area of Guizhou belongs to the lower Permian Liangshan Formation, and the sulfur content in coal varies widely from 0.90 to 16.65% (generally > 3%), with sulfides in the range of 0.80 to 4.60% (Zhou 2018). Coal mining activities have been carried out since the 1980s in this area, and most of the mines have been closed or abandoned now. According to the previous survey results, more than eighty abandoned coal mines were distributed along the river, and 24 of them produced acid mine water that is directly discharged into the river through unenclosed portals or alleys, with an annual discharge of about 56 million m^3, accounting for 43.26% of the total river flow (Li 2018). This provides an excellent opportunity to study the hydrochemical characteristics of regional abandoned coal mine drainage and the effects of AMD discharge on the local river hydrochemistry types and microbial community structure functions.

In this study, we analyzed the hydrochemical type and ion distribution characteristics of local abandoned coal mine drainage in the Pinglu River basin, which was a typical regional abandoned coal mine acidic drainage area, and explored the evolution process of hydrochemical type changes along the AMD receiving river. We also analyzed the impact of AMD influx on the microbial diversity, community structure and function of the river through high-throughput sequencing of river sediment microorganisms. The above studies lay the foundation for the ecological restoration of local rivers.

Materials And Methods

Sampling area

The study area is located in Kaili, Guizhou Province, Southwestern China, which belongs to the moderate humid monsoon climate zone of the central subtropics (Zhao 2008). The Lower Permian Liangshan Formation is the main coal-bearing stratum, containing bituminous coal with a thickness of 0.8-1.4 m. The rocks below the coal seam are bauxite and aluminous mudstone containing pyrite agglomerates or nodules, and the overly rocks are giant thick fine crystal tuff, and dense tuff interspersed with mud tuff and dolomitic tuff (Ren 2018). The local average multi-year rainfall is about 1264.7 mm, and a large amount of atmospheric precipitation with high dissolved oxygen infiltrates into the underground coal mining area, which, together with the groundwater rebounded into the abandoned coal mine, makes the underground coal mining area an area where complex physical, chemical and biological reactions of various pollutants occur (Chen et al. 2021b). As a result, pyrite in the coal seam and surrounding rocks will be oxidized, constituting a large amount of acid mine drainage overflowing from the coal mine portal, which in turn causes environmental pollution of surface water (Fig. 1). Large-scale AMD discharge, combined with the complex local karst landscape and hydrogeological conditions, has caused serious surface and groundwater pollution.

The abandoned coal mine drainage points were mainly distributed along the Pinglu River. After a comprehensive understanding of the hydrological conditions of the river and coal mines, we selected suitable sampling points to cover most of the drainage points and the river sections affected by them. We collected a total of twelve water samples (M1~M12) from the abandoned coal mine drainage along the Pinglu River, as showed in Fig. 1. The long-term discharge of AMD from the mine portal formed a distinct yellow or reddish-brown "pollution zone" in the

drainage runoff area, and some of the vegetation in the zone withered, indicating that the surface ecosystem was considerably inhibited. Large amount of AMD confluence was also seriously polluted the local river. We collected eight river water samples (R1~R8) and five sediment samples (S1~S5) of Pinglu River, covering both unpolluted and polluted sections of the river. Relatively clear water could be observed in the upstream section of the river, and the color of the river gradually turned to yellow at the confluence of AMD along the river and formed obvious red or yellow sediment on the riverbed. It can be observed from Fig. 1 that there is a significant difference in the color of water at the river crossings.

Sample collection

Collect each water sample using one 1.5 L pre-cleaned polyethylene bottle. The sediment samples were collected from the surface sediment of the river, and four subsamples were collected simultaneously near each sampling site and mixed homogeneously as representative samples for that site. The homogenized sediment samples were divided into two portions. The part for physical and chemical parameter testing was collected in the field and stored in a sampling box at 4°C and transported back to the laboratory for processing within 24 h. The sample for DNA extraction was stored in a sterile centrifuge tube at 4°C in the sampling box, completely frozen at -20°C, and transported on ice for storage at -80°C in the laboratory within 24 h until the next step of analysis.

Physicochemical analysis

The pH value of the water samples was evaluated in the field using a multi-function portable instrument (Shanghai Raytheon PHS-25). The collected water samples were returned to the laboratory as soon as possible and then filtered with the 0.45 μm polyester fiber filter membrane. Part of the filtered water samples were adjusted to acidity (pH<2) with HNO_3 for the determination of metal content by inductively coupled plasma mass spectrometry (ICP-MS), while another part of the water samples was directly tested for the other indicators. The concentrations of K^+ and Na^+ were measured by atomic absorption method (GFA-6880), Ca^{2+}, Mg^{2+} and HCO_3^- in the water samples were determined by chemical methods, and the anions Cl^- and SO_4^{2-} were evaluated by ion chromatography (ICS-Aquion).

The river sediment samples were freeze-dried by a freeze-dryer (FD-1A-50, BioCool, Beijing, China). Determination of pH value (Chen et al. 2021a)and total iron (Sun et al. 2018) in dry samples according to the reported method. The 0.2g dry samples after sieving through 0.15 mm mesh were digested in a microwave digestion bath and then determined by inductively coupled plasma mass spectrometry (ICP-MS, TFS, USA) for heavy metals Zn, Mn, Cd, Cu, and Cr (Lu et al. 2012). Total organic carbon (TOC), total nitrogen (TN) and total phosphorus(TP) in solid samples were measured by a K_2CrO_7-H_2SO_4 oxidation procedure (Perrier and Kellogg 1960), the Kjeldahl method (Zdravko et al. 2014) and NaOH fusion method (Xie et al. 2015), respectively. All measurements were performed in triplicate.

DNA extraction and Illumina MiSeq sequencing

Total DNA of the samples was extracted from 1.0g solid sample using the E.Z.N.A.® Soil DNA Kit (Omega Bio-tek, Norcross, GA, U.S.). For the extracted DNA, the concentration and quality were estimated by Nanodrop®ND-2000 UV-Vis Spectrophotometer (NanoDrop Technologies, USA). Amplification libraries were generated using the universal bacterial primers 338F and 806R for the V3-V4 region of the 16S rRNA gene (Lee et al. 2012). PCR extraction was carried out on 2% agarose gel, followed by purification of the extracted PCR using the AxyPrep DNA Gel Extraction Kit (Axygen Biosciences, Union City, CA, USA), and the concentration of PCR was quantified by QuantiFluor™-ST (Promega, USA).

The purified amplicons (300 bps paired) were sequenced on the Illumina MiSeq platform (Illumina, San Diego, USA) at Majorbio Bio-Pharm Technology Co. Ltd. (Shanghai, China). Sequences from the Illumina MiSeq platform were manipulated using the QIIME (v 1.9.1) package (Campbell et al. 2010). The raw fastq files were demultiplexed and quality controlled using Trimmomatic filtering, and then merged by FLASH (v 1.2.11) (Magoč and Salzberg 2011). Operational Taxonomic Unit (OTU) clustering was performed on the SILVA database with 97% similarity control according to the RDP classifier algorithm (v2.11) (Elmar et al. 2007).

Statistical analyses

Hydrochemical characteristics and the equivalent percentages of anions and cations of water samples were calculated using Schukalev classification method (Zhou and Ye 2014), and the Duove diagrams of the water samples were performed using AqQa software. The physicochemical parameters of the water samples were analyzed and clustered using the method of principal component analysis (PCA), and the saturation index of the water samples was calculated with the software PHREEQC (Juen et al. 2015)

The number of obtained OTU (Sobs), Chao1 (Chao 1984), Shannon (Shannon and Weaver 1950) and phylogenetic diversity were used to evaluate the diversity of bacterial communities of samples. Analysis of the river sediment samples was conducted by the Bray-Curtis Method (UPGMA) using Qiime and R language (V 3.3.1). Phylogenetic tree of the top OTUs was constructed based on the maximum likelihood method (ML) (Wim and Olivier 2005) and IQ-tree (v1.6.8). Differences in the distribution of top OTUs of upstream and downstream samples were compared and analyzed by Welch's t-test. For the annotated OTU matrix, the phenotype of the sample microbiome was predicted using the BugBase analysis tool (https://bugbase.cs.umn.edu/) (Ward et al. 2017). The above data was analyzed on the free online platform of Majorbio Cloud Platform (www.majorbio.com). Bubble plot and heat map were generated on an online platform for data analysis and visualization (http://www.bioinformatics. com.cn).

Results And Discussions

Physicochemical properties of samples

A total of twenty water samples, including twelve samples from the abandoned coal mine drainage (Group M, M1 ~ M12) and eight samples from Pinglu River (Group R, R1 to R8), were collected in our study. The comparison of the physicochemical parameters of the water samples from group M and group R is shown in Fig. 2. The pH value of Group M samples ranged from 2.78 to 7.57, and 58.3% (7 out of 12) of the samples have pH < 4.0. The continuous confluence of acidic drainage from abandoned coal mines has led to a gradual increase in the acidity of the Pinglu River from upstream to downstream, with the pH of the river decreasing from 8.16 (R1) in the upstream to a minimum of 3.22 (R5). Comparing with the surface water environmental quality standard (GB 3838 − 2002), the pH of river water in the middle and lower reaches of Pinglu River was significantly lower than the standard limit (6 ~ 9), indicating that the river had been seriously polluted by acidity. AMD from abandoned coal mines mainly originates from the oxidation of sulfide minerals (mainly pyrite) in coal and rocks in the underground mining area (Chen et al. 2021b), and a large amount of Fe, SO_4^{2-} and H^+ is generated during this oxidation process (Acharya and Kharel 2020). Water samples from abandoned coal mines drainage in our study also had high Fe and SO_4^{2-} contents, with average contents of 510.52 mg/L and 1954.29 mg/L, respectively, which were 8.25 and 4.96 times higher than those of river water samples. The content of metal ions such as Al, Mn, Zn and Cd in the abandoned coal mine drainage samples was significantly higher than that in the river samples (Fig. 2). In addition to metal ions, the Ca and Mg contents in the samples of group M were also significantly higher than those of group R ($p < 0.01$). Carbonate rocks

are widely distributed in the stratigraphic structure of this study area, with bauxite and bauxitic mudstone beneath the coal seam and fine-grained tuff and dolomitic tuff in the overlying rocks. During the formation and migration of AMD, these carbonate rocks were dissolved and released Ca^{2+} and Mg^{2+}, while the bauxite in the overlying rock released a large amount of Al ions, thus causing high Al content (average 100.81 mg/L) in the AMD from abandoned coal mines.

Principal component analysis (PCA) was performed on the physicochemical indicators of all water samples, and the proportion of the principal components PC1 and PC2 was 67.3% and 14.7%, respectively, with a total proportion of 82%, indicating that these two principal components can represent the overall distribution of the physicochemical indexes of water samples (Fig. 3). The green and yellow ellipses represent the 95% confidence intervals of the distribution of the samples in group R and group M, respectively. The existence of crossover areas in the grouped ellipses of the two groups of samples indicates that there is some similarity in the physicochemical indexes of the samples, especially the samples R5 ~ R8 in the downstream of the river, which are closer to the samples in group M, indicating that the physicochemical properties are more similar between them. As shown in Fig. 3(a), the upstream sample R1 is the farthest away from the group M samples, which indicates that there is a significant difference between the physicochemical properties of the unpolluted river section and samples from the abandoned coal mines drainage. Upstream samples of the river were characterized as weakly alkaline due to the wide distribution of carbonate minerals. However, pH value of the river gradually changed from weakly alkaline to acidic with the gradual convergence of AMD from abandoned coal mines along the river. From Fig. 3(a), it is obvious that the distance between the downstream samples (R5 ~ R8) and the abandoned coal mine drainage samples is gradually close to each other, which indicates that the physicochemical properties between the downstream samples and the abandoned coal mine drainage gradually tend to be similar. Comparing with the surface water quality standard (GB3838-2002), it can be seen that the concentration of total Fe and SO_4^{2-} in the middle and downstream samples of the river all exceeded the limits, except for the upstream samples R1 ~ R3. Especially for samples R4 and R5, with the confluence of M6 (pH 3.21) and M7 (pH 4.20), the concentration of total Fe and SO_4^{2-} of the river increased rapidly from 1.86 mg/L to 100.00 mg/L, and 285.00 mg/L to 542.00 mg/L, respectively, while the pH value of the river also plummeted from 6.23 to 3.22. From the clustering of the samples in group M, samples with pH < 4.0 are more aggregated with each other, indicating that the physicochemical properties of the strongly acidic drainage were more similar. As demonstrated in Fig. 3(b), these strongly acidic drainage samples were mainly distributed in the negative half-axis of the PC1 axis, which indicates that their distribution was negatively correlated with pH and Na^+ and positively correlated with other indicators. Samples with pH > 5.5 in group M (M1, M5 and M9) and river samples (group R) were all distributed in the positive half-axis of the PC1 axis, indicating that the distribution of these samples was positively correlated with pH and Na^+.

We collected five sediment samples from the upstream to downstream of Pinglu River, and the physicochemical properties of the solid samples are shown in Table 1. As the pH value of the river rapidly decreased with the confluence of AMD from abandoned coal mines, resulting in a gradual decrease in the pH of the river sediment from weakly alkaline (pH > 8.0) to neutral (Table 1). The variation of pH in river sediment is significantly smaller than that of the river water samples, which may be due to the widespread distribution of carbonate rocks, where alkaline minerals in the riverbed neutralize part of the acidity of river, resulting in the pH value of downstream river sediment remaining neutral. The total Fe content of river sediment samples ranged from 31.36 to 63.60 mg/g (average 45.06 mg/g).

Table 1
Physicochemical properties of river sediment samples

Samples	pH	TOC	TP	TN	Fe	Mn	Zn	Cd	Cu	Cr
		mg/g	mg/g	mg/g	mg/g	mg/kg	mg/kg	mg/kg	mg/kg	mg/kg
S1	8.00	12.68	0.55	1.76	37.52	459.00	143.00	1.04	33.10	188.00
S2	8.14	8.12	0.58	1.13	31.36	660.00	84.20	0.35	23.80	96.40
S3	7.78	13.90	0.34	0.85	55.16	417.00	77.90	0.91	17.90	90.60
S4	7.76	15.56	0.41	1.49	37.66	432.00	85.10	1.16	20.20	160.00
S5	7.16	19.95	0.17	1.72	63.60	440.00	140.00	1.13	20.90	81.10

Hydrochemical types of water samples collected from different regions

We collected a total of twenty water samples from different regions of the study area. Results of physicochemical properties showed that the pH values of the twelve abandoned coal mines drainage samples ranged from 2.78 to 7.57, and the concentration of the major cations Ca^{2+} 108.85 ~ 317.17 mg/L (average 226.56 mg/L), Mg^{2+} 126.26 ~ 133.33 mg/L (average 79.60 mg/L), K^{+}+Na^{+} 3.06 ~ 20.33 mg/L (average 12.04 mg/L), and the main anion $SO4^{2-}$ ranged from 248.39 to 3430.77 mg/L with the average concentration 1954.29 mg/L, showing an overall characteristic of high Ca-Mg and high sulfate (Fig. 4(a)). According to the Shukarev classification (Zhou and Ye 2014), hydrochemical types of the abandoned coal mine drainage were all SO_4-Ca·Mg types, except M1 which was SO_4-Ca type (Table 2). The pH range of Pinglu River water samples was 3.22 ~ 7.65, Ca^{2+} 54.25 ~ 239.21 mg/L (average 115.79 mg/L), Mg^{2+} 13.3 ~ 39.29 mg/L (average 25.15 mg/L), K^{+}+Na^{+} 5.58 ~ 8.67 mg/L (average 7.324 mg/L), and the quality of the river showed high calcium and magnesium content characteristics. The concentration of the main anions SO_4^{2-} ranged from 47.35 to 846.15 mg/L (average 393.83 mg/L) and HCO_3^{-} 0.00 ~ 152.55 mg/L (average 59.49 mg/L). The distribution of anions along the river showed that anions in the upstream samples of the river (R1 and R2) were dominant by HCO_3^{-}, while SO_4^{2-} was the main anion in downstream samples (R3 ~ R8) (Fig. 4(b)). Shukarev classification calculation showed that the hydrochemical types of the Pinglu River from upstream to downstream were SO_4·HCO_3-Ca·Mg (R1), SO_4·HCO_3-Ca (R2 and R3), SO_4-Ca (R4) and SO_4-Ca·Mg (R5 ~ R8) in order (Table 2).

Table 2
Percentage of anion and cation equivalents and hydrochemical types of water samples

Samples	Ca^{2+}	Mg^{2+}	Na^{+}	K^{+}	HCO_3^{-}	SO_4^{2-}	Cl^{-}	Hydrochemical type
M1	77.81	20.58	0.39	1.22	0.56	98.33	1.11	SO_4-Ca
M2	64.74	32.64	0.54	2.08	0.00	99.02	0.98	SO_4-Ca·Mg
M3	62.28	35.80	0.40	1.51	0.00	99.39	0.61	SO_4-Ca·Mg
M4	64.06	33.38	0.42	2.15	0.35	98.23	1.42	SO_4-Ca·Mg
M5	70.18	28.18	1.14	0.50	21.99	75.82	2.20	SO_4-Ca·Mg
M6	60.53	36.68	0.57	2.22	0.00	98.72	1.28	SO_4-Ca·Mg
M7	63.58	35.96	0.34	0.12	0.00	99.65	0.35	SO_4-Ca·Mg
M8	62.33	35.61	0.38	1.69	0.00	99.59	0.41	SO_4-Ca·Mg
M9	60.44	38.45	0.32	0.80	0.00	97.80	2.20	SO_4-Ca·Mg
M10	59.09	39.13	0.46	1.32	0.00	99.14	0.86	SO_4-Ca·Mg
M11	59.27	39.31	0.33	1.08	0.00	99.05	0.95	SO_4-Ca·Mg
M12	49.19	48.40	0.34	2.07	0.00	99.31	0.69	SO_4-Ca·Mg
R1	65.19	26.64	6.51	1.66	69.48	25.38	5.14	SO_4·HCO_3-Ca·Mg
R2	71.25	24.68	2.72	1.35	51.29	41.54	7.17	SO_4·HCO_3-Ca
R3	76.20	20.53	2.24	1.03	30.04	65.23	4.73	SO_4·HCO_3-Ca
R4	75.07	22.43	1.40	1.11	8.88	88.16	2.96	SO_4-Ca
R5	68.95	27.94	1.81	1.30	0.00	96.59	3.41	SO_4-Ca·Mg
R6	69.13	28.78	0.96	1.14	0.00	96.81	3.19	SO_4-Ca·Mg
R7	71.45	25.87	1.38	1.30	0.85	95.33	3.82	SO_4-Ca·Mg
R8	71.47	26.26	1.16	1.11	0.00	97.70	2.30	SO_4-Ca·Mg

Unit %

With the confluence of abandoned coal mines drainage with low pH and high content of sulfate, hydrochemical types of the Pingly River gradually changed from SO_4·HCO_3-Ca·Mg to SO_4-Ca·Mg type. Meanwhile, the total dissolved solids (TDS) and hardness of river gradually increased, with TDS increasing from 296.70 mg/L to 1083.54 mg/L, and the hardness of river (calculated by $CaCO_3$ content) increasing from 190.24 mg/L to 553.74 mg/L. According to the classification of river hardness, the quality of river from upstream to downstream of Pinglu River gradually changed from medium hard to high hard. Villages and farmlands are distributed along the river, and most of the local farmlands were irrigated by water diverted from the Pinglu River. According to the calculation results of Aq-QA

software, the irrigation risk of the upstream section of Pinglu River (R1~R4) was medium, while the section from R5 onwards has become high risk, which indicates that the downstream section of river was not suitable for agricultural irrigation. Irrigating farmland with such extreme hardness and mineralization river water can cause significant changes in soil properties, such as soil slumping or salinization, etc.

Revealing the evolution of ion concentration in different types of water samples

Atmospheric precipitation and groundwater rebound are the main sources of mine water in abandoned coal mines, so the local stratigraphic and hydrodynamic conditions can significantly affect the hydrochemical characteristics of mine water. The coal-bearing strata in the Yudong River basin belong to the Lower Permian Liangshan Formation, and the stratigraphic structure mainly consists of quartz sandstone, carbonaceous tuff, coal seams, and bauxite intercalated with pyrite agglomerates or nodules, and the thickness of iron-bearing ore layers below the coal seams is about 0 ~ 1.5m (Li 2018). After the abandonment of underground coal mines, the oxidized pyrite in the rock strata will produce a large amount of H^+ and SO_4^{2-}, resulting in the decomposition of HCO_3^- to CO_2 under acidic conditions, so SO_4^{2-} becomes the main anion in coal mine drainage, accounting for 75.82 ~ 99.65% (average 97.00%) of the equivalent percentage. As the comprehensive index reflecting water quality, the TDS of abandoned coal mine drainage ranged from 488.46 to 5125.87 mg/L with an average of 2909.37 mg/L, of which 66.67% (8 out of 12 water samples) exceeded the groundwater V quality standard. The fitted results (Fig. 5(a)) showed a significant positive correlation between TDS and SO_4^{2-} in coal mine drainage ($p < 0.05$) with a correlation coefficient of 0.996, indicating that sulfate is the main factor affecting the overall water quality, which further elucidates that the oxidation of pyrite in abandoned coal mines is the main cause of AMD pollution in this area.

The cations in the coal mine drainage are mainly Ca^{2+} and Mg^{2+}, with Ca^{2+} accounting for 49.19 ~ 77.81% (average 62.79%) of the equivalent percentage, Mg^{2+} 20.58 ~ 48.40% (average 35.34%), and Na^++K^+ ranging from 0.45 to 2.78%. Local carbonate rocks containing calcium and magnesium (such as dolomite and dolomitic limestone) are widely distributed (Wang et al. 2009). Therefore, the dissolution and weathering of such kind of carbonate rocks under natural conditions is the primary source of Ca^{2+} and Mg^{2+} in coal mine drainage. Although Ca^{2+} and Mg^{2+} are the principal cations in coal mine drainage, their distribution in different coal mine drainage samples varies. For example, the percentages of Ca^{2+} and Mg^{2+} in the M1 were 77.81% and 20.58%, respectively, while they were 49.19% and 48.40% in M12 (Table 1). Ratios of Ca/Mg in M1 and M12 samples were 6.30 and 1.69, respectively. Results showed that the Ca/Mg ratio in coal mine drainage was significantly negatively correlated with the concentration of SO_4^{2-} ($p < 0.05$), i.e., the Ca/Mg ratio decreased with the increase of SO_4^{2-} concentration (Fig. 5 (b)). This is probably because the solubility product of $CaSO_4$ is smaller than that of $MgSO_4$, and when the water contains a large amount of SO_4^{2-} and Ca^{2+}, Ca^{2+} will first reach saturation and form precipitation, thus leading to the decrease in the proportion of Ca^{2+}, while on the contrary the percentage of Mg^{2+} will increase, eventually leading to the decrease of the Ca/Mg ratio. The saturation indices of the water samples were calculated by PHREEQC, and the calculation results showed that the saturation indices of Anhydrite ($CaSO_4$) and Gypsum ($CaSO_4.2H_2O$) in the water samples of group M were all exceeded zero, indicating a supersaturated state, while the saturation indices of Halite (NaCl) and Sylvite (KCl) were all below zero, indicating a dissolved state (Table 3).

Table 3
Mineral saturation index of water samples collected from abandoned coal mines

Sample	M1	M2	M3	M4	M5	M6	M7	M8	M9	M10	M11	M12
$CaSO_4$	1.42	1.79	1.85	1.49	0.89	1.53	1.64	1.92	1.15	1.86	1.87	1.95
$CaSO_4 \cdot 2H_2O$	1.71	2.06	2.11	1.77	1.19	1.82	1.93	2.18	1.44	2.13	2.14	2.20
NaCl	-7.11	-6.51	-6.79	-6.77	-6.93	-6.60	-7.29	-6.90	-7.06	-6.52	-6.60	-6.61
KCl	-5.84	-5.25	-5.56	-5.33	-6.45	-5.28	-7.01	-5.60	-5.91	-5.40	-5.41	-5.18

Among the cations in river samples, Ca^{2+} was absolutely dominant, with its equivalent percentage ranging from 65.19 to 76.20% (average 71.09%), Mg^{2+} from 20.53 to 28.78% (average 25.39%), while $Na^{+}+K^{+}$ together accounted for the least (2.10 to 8.17%, average 3.52%). Dissolved weathering of the widely distributed carbonate minerals was the direct source of Ca^{2+} and Mg^{2+} (Wang et al. 2009), thus making the cations in the river water to be dominated by "Ca and Mg". The concentration of Ca^{2+} and Mg^{2+} in the water samples from upstream to downstream of Pinglu River increased linearly, where Ca^{2+} increased from 54.25 mg/L (R1) to 162.63 mg/L (R8) and Mg^{2+} increased from 13.30 mg/L (R1) to 35.86 mg/L (R8). Previous investigations showed that the total annual discharge of abandoned coal mines accounted for about 43.26% of the total river flow, and the confluence of such coal mine discharges with high calcium and magnesium concentrations (average 226.56 mg/L and 79.60 mg/L, respectively) significantly increased the calcium and magnesium contents in the river. In addition, the confluence of large amounts of acidic coal mine drainage significantly reduced the pH value of the river, which further accelerated the dissolution weathering of carbonate minerals such as dolomite and calcite. Correlation analysis showed that the concentrations of Ca^{2+} and Mg^{2+} in the river were significantly negatively correlated with pH ($p<0.05$) with correlation coefficients of -0.860 and -0.886, respectively, which further indicated that the changes of hydrochemical characteristics in Pinglu River were mainly related to the confluence of abandoned coal mine drainage along the river. The Ca/Mg ratios of river samples ranged from 4.00 to 6.19. Unlike lower Ca/Mg ratios of abandoned coal mine drainage under acidic conditions (all less than 3.0), the Ca/Mg ratios of the downstream section (R5~R8) of the river all exceeded 4.0 despite their lower pH values. Statistical analysis showed no significant correlation between Ca/Mg ratio and the concentration of SO_4^{2-} in river samples. The anions in river samples were mainly dominated by HCO_3^{-} and SO_4^{2-}, and their distribution on the upstream and downstream river was significantly different. HCO_3^{-} was the principal anion in the upstream sample R1, accounting for 69.48% of the equivalent percentage. Since HCO_3^{-} is easily to be decomposed under acidic conditions, its equivalent percentage in the water samples gradually decreases with the decrease of pH values, resulting in its percentage at R2 and R3 has been reduced to 51.29% and 30.04%, respectively, especially in the downstream samples, the percentage of HCO_3^{-} has been reduced to less than 1%. In contrast, the equivalence percentages of SO_4^{2-} in the river gradually increased from upstream to downstream, with their equivalent percentage in the upstream samples R1 and R2 being 25.38% and 41.54%, respectively, while they were all >95% in downstream river samples (R5 to R8).

Overall bacterial community taxonomic compositions of river sediment

A total of 254,678 valid reads were defined in five sequencing libraries with an average length of 421 bp. Based on the 97% similarity threshold, all sequences were finally clustered into 2,844 operational taxonomic units (OTUs), ranging from 1758 to 2430. The highest number of OTUs was obtained from the upstream sample R1, and the

number of OTUs obtained in river sediment gradually decreased from upstream to downstream, especially at R5, the most polluted point, was only 1758. The alpha diversity index Chao1 and Phylogenetic diversity also showed the same tendency (Fig. 6), which indicated that the richness of microorganisms in the river sediments gradually decreased from upstream to downstream. This may be due to the fact that the confluence of acidic mine drainage along the Pinglu River changed the living conditions of microorganisms and inhibited the survival of some of them. The Shannon index of sample R5 was significantly lower than the other samples, indicating the lowest bacterial diversity.

A total of 40 phyla were identified from the sediment samples. The relative abundance of the top 15 most dominant phyla are shown in Fig. 7(a). Among these samples, *Chloroflexi* was the most abundant phylum, constituting in average of 23.93% of the total sequence reads (11.53 ~ 37.76% in all samples). *Proteobacteria*, *Actinobacteriota* and *Acidobacteriota* ranked as the following three most abundant phyla, accounting for 21.45% (17.19 ~ 26.96% in all samples), 17.38% (11.72 ~ 31.39% in all samples), and 14.23% (9.60 ~ 18.01% in all samples) of the total reads, respectively. Phyla with relative abundance > 5% in at least one sample included *Desulfobacterota* and *Firmicutes* with the average relative abundance of 3.28% (0.62 ~ 5.83% in all samples) and 2.97% (0.60 ~ 5.39% in all samples), respectively. The remaining 34 phyla accounted for about 16.76% of the total reads. The distribution of the dominant phylum varied among samples, except for the downstream S5 sample, where the dominant phylum was *Actinobacteriota* (31.39% relative abundance) and the subdominant phylum was *Proteobacteria* (26.96% relative abundance); the dominant phylum from S1 to S4 was *Chloroflexi* (20.61%~37.76% relative abundance) and the subdominant phylum was *Proteobacteria* (19.95%~22.44% relative abundance). The relative abundance of the dominant phylum *Chloroflexi* in the sediments from upstream to downstream of the river showed an increase followed by a decrease. At the class level, a widely variety of classes dominated. Among them, the most abundant classes were *Alphaproteobacteria, Vicinamibacteria, Gammaproteobacteria, Anaerolineae, Actinobacteria*, and *Thermoleophilia*, accounting for 11.52%, 10.00%, 9.93%, 9.12%, 6.28% and 6.14% of the total reads, respectively.

At the genus level, the detailed information about the relative abundance of the top 35 genera is indicated in Fig. 8. Clearly, the dominant genera in the sediment samples included *Gaiella, Geobacter, Sphingomonas, MND1* and *Anaeromyxobacter* etc., with the average relative abundance of 2.65%, 1.19%, 1.06%, 0.99% and 0.92%, respectively. The clustering of the relative abundance of the top 35 genera in the samples is shown in Fig. 7(b), where red represents the genera with higher relative abundance in the samples, and blue for genera with lower relative abundance. Results showed that the distribution of these 35 top genera along the river clustered in separate groups. Genera with high abundance (relative abundance > 1.0%) in the upstream sample S1 included *Geobacter, Marmoricola, Ellin6067, Phycicoccus* and *Nocardioides*, mainly belonging to the phylum *Actinobacteriota* and *Proteobacteria*. *Geobacter* had the highest percentage (3.82%) among all the major genera of S1 samples, which are one kind of heterotrophic iron-reducing bacterium (Islam et al. 2005). *Marmoricola* is the second most abundant genus in S1 (3.35%), which is a Gram-positive and aerobic bacterium with the suitable pH range of 6 ~ 9, belonging to the member of the family *Nocardioidaceae* (Schumann et al. 2018). *Anaeromyxobacter* and *Arthrobacter* were genera with relatively high abundance in sample S2, where *Anaeromyxobacter* is an aryl-halorespiring facultative anaerobic myxobacterium, and some studies have demonstrated that bacteria of this genus have the ability to reduce iron and U(VI) metal. For example, some species can grow with the mineral hematite, an insoluble form of ferric iron, as electron acceptor (Chao 2011). *Arthrobacter* is one kind of the basic bacterium in soil and some species of this genus have the potential to remediate polluted environments by reducing hexavalent chromium and degrading agricultural pesticides, as well as by their ability to remediate nitrogen (Fu et al. 2014). The distribution of major genera in sample S3 was somewhat analogous to that of S2. *Nordella, Clostridium_sensu_stricto_1, Hyphomicrobium* and *Acidaminobacter* were more abundant in S3 and S2 than in the other samples, and the other

genera with relatively high abundance in S3 also included *Bryobacter, Candidatus_ Alysiosphaera, Pedomicrobium* and *FFCH7168*. *Pedomicrobium* belongs to class *Alphaproteobacteria*, and acts as a terrestrial polarophilic bacterium. This kind of bacteria can inhabit particularly harsh environments and the strain *Pedomicrobium manganicum* has the ability to oxidize manganese and is usually used in many bioremediation processes, such as the removal of manganese from water purification systems (Zhao et al. 2019). *Haliangium, Citrifermentans* and *Nitrospira* were relatively abundant in the sample S4. Among them, *Haliangium*, a rod-shaped myxobacterium, commonly found in the ocean, being a class of an obligate halophile (Sun et al. 2016b). The major genera in S5 differed greatly from the other samples, and the genera with relative abundance > 1% included *Gaiella, Sphingomonas, MND1, Pseudolabrys, Bradyrhizobium, Bacillus*, etc. These genera mainly belong to the *Proteobacteria*. Previous studies have demonstrated that the abundance of *Proteobacteria* increases in soil contaminated by AMD (Chen et al. 2021b), and the relative abundance of *Proteobacteria* was also highest in the extremely contaminated downstream sample S5 in our study with the relative abundance of 26.96%. *Gaiella*, the dominant genus in river sediment, had the highest abundance in the sample S5 (relative abundance 6.16%) and is an aerobic heterotrophic bacterium (Albuquerque et al. 2011). In conclusion, most of the microorganisms in the sediment of Pinglu River are heterotrophic, and some genera can participate in the metabolic processes of Fe, Mn and N, which have the potential to remediate the polluted environment.

Differences of microbial communities in river sediments of different section

The similarity of microbial communities in river sediment was assessed using cluster analysis. As shown in Fig. 9, the clustering analysis revealed that the bacterial communities of the samples could be clustered into two groups. The first group contains upstream samples S1 to S3, and the second group includes downstream samples S4 and S5. General taxonomic pattern in Fig. 9 was driven primarily by differences in abundance of the major taxonomic groups.

As shown in Fig. 8, genera such as *Geobacter*, *Anaeromyxobacter*, *Marmoricola* and *Phycicoccus*, accounted for relatively high properties in upstream samples, and *Gaiella*, *MND1* and *Pseudolabrys* appeared to be more abundant in the downstream samples. The phylogenetic distance among the top 30 abundant OTUs and their significant differences in upstream and downstream samples was also shown in Fig. 10. These 30 major OTUs were mainly distributed in *Proteobacteria* and *Actinobacteriota* with a proportion of 50% (15 out of 30) and 30% (9 out of 30), respectively, while other phyla also included *Desulfobacterota, Firmicutes* and *Myxococcota*. Figure 10 shows both the variation in the distribution of these 30 OTUs in upstream and downstream samples, where blue represents upstream samples and yellow for downstream samples. There are 14 top OTUs mainly distributed in upstream samples, of which five of them belong to *Proteobacteria* (35.71%), five to *Actinobacteriota* (35.71%), two to *Desulfobacterota* (14.28%), one to *Firmicutes* (7.14%) and one to *Myxococcota* (7.14%). The other 16 top OTUs were mainly distributed in the downstream samples, of which ten belonged to *Proteobacteria* (62.5%), four to *Actinobacteriota* (25%), one to *Desulfobacterota* (6.25%) and one to *Myxococcota* (6.25%). Core genera of the upstream samples were mainly attributed to *Proteobacteria* and *Actinobacteriota*, while for downstream samples, were mainly attributed to *Proteobacteria*. Significant difference analysis based on Welch's t-test showed that significantly different genera for upstream samples were *Phycicoccus* (OTU1130) and *Ellin6067* (OTU1354), while *Pseudolabrys* (OTU5585) and *Dongia* (OTU2735) were the most different genera in the downstream samples.

Phenotypic prediction of microbial communities in river sediments

To gain insight into the functions of the bacterial community, we used BugBase, a bioinformatics tool that can infer the phenotypes of the entire community based on 16S rRNA gene (Lucas et al. 2018). A total of nine phenotypes were predicted for the microbial communities of the river sediment samples, including Aerobic, Anaerobic, Contains Mobile Elements, Facultatively Anaerobic, Forms Biofilms, Gram Negative, Gram Positive, Potentially Pathogenic and Stress Tolerant, and the relative abundance distribution of each phenotype in samples was predicted (Fig. 11(a)). Results of the BugBase prediction revealed that the microorganisms in river sediment samples were predominantly Gram-negative bacterium (average relative abundance 71.40%), while Gram-positive bacterium only accounted for 28.60% of the total community. In terms of oxygen utilization by microorganisms, the river sediment was mostly composed of aerobic microorganisms with the average relative abundance of 51.63%, while anaerobic microorganisms only accounted for 19.37% of the community. Comparing the distribution proportion of microorganisms in samples along the river (Fig. 11(b)), we found that the abundance of anaerobic microorganisms in river sediment showed a gradual decrease from upstream to downstream, from 24.77% (S1) to 12.46% (S5), while the abundance of aerobic microorganisms was basically stable from upstream to midstream, and gradually increased from midstream to downstream, from 47.50% (S3) to 60.79% (S5). To clarify the reasons for the differences between aerobic and anaerobic phenotypes in samples, we statistically analyzed the contribution of the major genera to the aerobic and anaerobic phenotypes in samples, as shown in Fig. 11(c) and Fig. 11(d), respectively. It can be seen that the aerobic phenotypes in samples were mainly contributed by genera *Gaiella, Marmoricola, Sphingomonas, Anaeromyxobacter, Bryobacter* and *Nocardioide*s, with the average relative abundances of 1.84%, 1.48%, 1.14%, 1.12%, 0.82% and 0.81%, respectively. Among them, *Gaiella* and *Sphingomonas* were mainly distributed in downstream samples, while *Marmoricola, Anaeromyxobacter, Bryobacter* and *Nocardioides* were mainly distributed in upstream samples. The anaerobic phenotypes in samples were mainly contributed by genera *Geobacter, Citrifermentans, Luteitalea* and *Vicinamibacter*, with the average relative abundances of 1.34%, 0.31%, 0.26% and 0.18% in samples, respectively. Among them, *Geobacter, Luteitalea* and *Vicinamibacter* were mainly distributed in upstream samples, while *Citrifermentans* was mainly distributed in downstream samples.

Influence of physicochemical properties on microbial communities of river sediment

The distribution of microbial communities and diversity in sediments was closely related to environmental factors. Results of the Partial Mantel test based on Bray Curtis distance algorithm showed that the microbial communities in sediment samples were mainly attributed to pH, TOC and TP with correlation coefficients of 0.736, 0.607 and 0.564, respectively, and the absolute values of correlation coefficients between other physicochemical factors and microbial communities were all below 0.50. Figure 12 showed the correlation coefficients between the main genera and alpha diversity indicators in samples and the three main environmental factors, with red representing positive correlation and blue for negative correlation. Correlation coefficients of community richness index Chao1 with pH, TOC and TP was 0.849, 0.636 and 0.813, respectively, which was significantly positively with the other two indices except TOC ($p < 0.05$). The microbial richness of river sediment gradually decreased from upstream to downstream, which was consistent with the trend of pH and TP. The community diversity index Shannon showed significant positive correlations ($p < 0.05$) with pH, TOC and TP, with correlation coefficients of 0.914, 0.782 and 0.782, respectively. The distribution of *Geobacter, Anaeromyxobacter, Marmoricola, Ellin6067, Phycicoccus, Arthrobacter* and *Ilumatobacter* among the main sediment genera was positively correlated with pH and TP, and these genera were mainly were mainly distributed in the upstream samples. The richness of these genera gradually decreased from upstream to downstream as the pH and TP reduced in river sediment. In the downstream of the river, these genera were gradually replaced by *Gaiella, Sphingomonas, MND1, Pseudolabrys, Pedomicrobium, Bradyrhizobium* and *mle1-7*, which showed negative correlations with pH and TP.

Conclusions

In the present study, we aimed to more accurately discover the hydrochemical characteristic and microbial community evolution of the river affected by regional abandoned coal mine drainage, mainly included:

(1) The abandoned coal mine drainage showed characteristics of strong acidity, high Ca and Mg content and high sulfate, with SO_4-Ca·Mg as the main hydrochemical type. Correlation analysis indicated that the Ca/Mg ratio of AMD from abandoned coal mines was significantly negatively correlated with SO_4^{2-} ($R^2 = 0.612$, $p < 0.05$).

(2) With the confluence of AMD from abandoned coal mines along the river, the river gradually changed from weakly alkaline (pH 8.16) to strongly acidic (pH 3.22 at minimum), and the hydrochemical type of the river gradually changed from SO_4·HCO_3-Ca·Mg to SO_4-Ca·Mg, accompanied by a gradual decrease in the richness and diversity of microbial communities in the river sediments during this process. The pH of river sediment varied less than that of river water and showed neutral to weak alkalinity overall.
(3) The dominant phyla in the sediment included *Chloroflexi, Proteobacteria, Actinobacteriota* and *Acidobacteriota*, with the average relative abundance of 23.93%, 21.45%, 17.38% and 14.23%, respectively. The dominant genera in river sediment mainly included *Gaiella, Geobacter, Sphingomonas, MND1* and *Anaeromyxobacter* etc. Welch's t-test revealed significant differences in microbial communities between upstream and downstream sediments, with the upstream samples mainly distributed in the *Proteobacteria* and *Actinobacteriota* phyla, while for downstream samples, were *Proteobacteria* phylum, with *Phycicoccus, Ellin6067, Pseudolabrys* and *Dongia* as the main differential genera. Correlation analysis between environmental factors and microbial communities indicated that the distribution of microbial communities in sediments was mainly affected by pH, TOC and TP.
(4) In addition, we predicted the microbial community function by BugBase phenotype prediction method, and results showed that the microorganisms in the sediment mainly consisted of aerobic microorganisms (average relative abundance 51.63%), while anaerobic microorganisms only accounted for 19.37%, and the abundance of anaerobic microorganisms in the sediment from upstream to downstream was characterized by a gradual decrease from 24.77–12.46%, which was mainly contributed by genera such as *Geobacter, Citrifermentans, Luteitalea* and *Vicinamibacter* etc.

Declarations

Ethics approval and consent to participate: Not applicable.

Consent for publication: Not applicable.

Availability of data and materials: Availability of data and materials will be available upon request.

Competing interests: The authors declare no competing interests.

Funding: This work was financially supported by the National Natural Science Foundation of China (No. 41977159) and the Open Funding of CNACG Key Laboratory of Mineral Resources (NO. KFKT-2020-3).

Author contribution

All authors contributed to the study conception and design. Material preparation, data collection, and analysis were performed by Di Chen, Yun Zhang, and Qiyan Feng. The first draft of the manuscript was written by Di Chen and all authors commented on previous versions of the manuscript. All authors read and approved the final manuscript.

Acknowledgements

The authors thank the financial support from the National Natural Science Foundation of China (grant No. 41977159), and the Open Fund of CNACG Key Laboratory of Mineral Resources in Coal Measures (No. KFKT-2020-3).

References

1. Acharya BS, Kharel G (2020) Acid mine drainage from coal mining in the United States–An overview. J Hydrol 588:125061
2. Akcil A, Koldas S (2005) Acid Mine Drainage (AMD): causes, treatment and case studies. J Clean Prod 14:1139–1145
3. Albuquerque L, França L, Rainey FA et al (2011) *Gaiella occulta gen. nov., sp. nov.*, a novel representative of a deep branching phylogenetic lineage within the class *Actinobacteria* and proposal of *Gaiellaceae fam. nov.* and *Gaiellales ord. nov*. Syst Appl Mocrobiol 34:595–599
4. Campbell BJ, Polson SW, Hanson TE et al (2010) The effect of nutrient deposition on bacterial communities in Arctic tundra soil. Environ Microbiol 12:1842–1854
5. Chao A (1984) Non-parametric Estimation of the Number of Classes in a Population. Scand J Stat 11:265–270
6. Chao Z (2011) Variation of *Anaeromyxobacter* community structure and abundance in paddy soil slurry over flooding time. Afr J Agric Res 28:6107–6118
7. Chen D, Feng Q, Li W et al (2021a) Effects of acid drainage from abandoned coal mines on the microbial community of Shandi River sediment, Shanxi Province. Int J Coal Sci Technol 8:756–766
8. Chen D, Feng Q, Liang H (2021b) Effects of long-term discharge of acid mine drainage from abandoned coal mines on soil microorganisms: microbial community structure, interaction patterns, and metabolic functions. Environ Sci Pollut R 28:53936–53952
9. Elmar P, Christian Q, Katrin K et al (2007) SILVA: a comprehensive online resource for quality checked and aligned ribosomal RNA sequence data compatible with ARB. Nucleic Acids Res 35:7188–7196
10. Feng Q-Y, Zhou L (2016) Risk assessment and control of groundwater pollution in abandon mine. China Environmental Science Press, Beijing. (in Chinese)
11. Fu HL, Wei YF, Zou YY et al (2014) Research Progress on the *Actinomyces arthrobacter*. Adv Microbiol 04:747–753
12. Islam FS, Boothman C, Gault AG et al (2005) Potential role of the Fe(III)-reducing bacteria *Geobacter* and *Geothrix* in controlling arsenic solubility in Bengal delta sediments. Mineral Mag 69:865–875
13. Juen LL, Aris AZ, Shan NT et al (2015) Geochemical Modeling of Element Species in Selected Tropical Estuaries and Coastal Water of the Strait of Malacca. Procedia Environ Sci 30:109–114
14. Lee CK, Barbier BA, Bottos EM et al (2012) The Inter-Valley Soil Comparative Survey: the ecology of Dry Valley edaphic microbial communities. Isme J 6:1046–1057
15. Lucas SK, Yang R, Dunitz JM et al (2018) 16S rRNA gene sequencing reveals site-specific signatures of the upper and lower airways of cystic fibrosis patients. J Cyst Fibros 17:204–212
16. Lu Z-L, Hu H-Y, Yao H (2012) Study on Quantitative Analysis Method for Several Heavy Metals in Soil Sample by Inductively Coupled Plasma-Mass Spectrometry. Rock and Mineral Analysis 31:241–246 (in Chinese)

17. Magoč T, Salzberg SL (2011) FLASH: fast length adjustment of short reads to improve genome assemblies. Bioinformatics 27:2957–2963
18. Perrier ER, Kellogg M (1960) Colorimetric determination of soil organic matter. Soil ence 90:104–106
19. Ren H-J (2018) Study on water pollution problem of Kaili Longdongquan in Guizhou. Coal and Chemical Industry 41:56–58 (in Chinese)
20. Schumann P, Zhang DC, Franca L et al (2018) *Marmoricola silvestris* sp nov., a novel actinobacterium isolated from alpine forest soil. Int J Syst Evol Micr 68:1313–1318
21. Shannon C, Weaver W (1950) The Mathematical Theory of Communication. Phys Today 3:31
22. Sun W, Xiao E, Krumins V et al (2016a) Characterization of the microbial community composition and the distribution of Fe-metabolizing bacteria in a creek contaminated by acid mine drainage. Appl Microbiol Biot 100:8523–8535
23. Sun W, Xiao E, Pu Z et al (2018) Paddy soil microbial communities driven by environment and microbe-microbe interactions: A case study of elevation-resolved microbial communities in a rice terrace. Sci Total Environ 612:884–893
24. Sun Y, Tomura T, Sato J et al (2016b) Isolation and Biosynthetic Analysis of Haliamide, a New PKS-NRPS Hybrid Metabolite from the Marine *Myxobacterium Haliangium* ochraceum. Molecules 21:59
25. Wang J-B, Zhu L-P, Ju J-T et al (2009) Water Chemistry of Eastern Nam Lake Area and Inflowing Rivers in Tibet. Scientia Geogr Sinica 29:288–293 (in Chinese)
26. Ward T, Larson J, Meulemans J et al (2017) BugBase Predicts Organism Level Microbiome Phenotypes. 133462
27. Wim H, Olivier G (2005) Improving the efficiency of SPR moves in phylogenetic tree search methods based on maximum likelihood. Bioinformatics 21:4338–4347
28. Xie LW, Zhong J, Cao FX et al (2015) Evaluation of soil fertility in the succession of karst rocky desertification using principal component analysis. Solid Earth 6:3333–3359
29. Yuan L (2019) Promote the precise development and utilization of closed/abandoned mine resources in China. Coal Economic Research 39:1 (in Chinese)
30. Zdravko P, Traj ES, Ivana VK et al (2014) Study of nitrogen pollution in Croatia by moss biomonitoring and Kjeldahl method. Environ Lett 49:1402–1408
31. Zhao X, Liu B, Wang X et al (2019) Single molecule sequencing reveals response of manganese-oxidizing microbiome to different biofilter media in drinking water systems. Water Res 171:115424
32. Zhao H-X (2008) Analysis of coal mine wastewater pollution in Kaili area and experimental study of microbial treatment. Dissertation, Guizhou University. (in Chinese)
33. Zhang Q-X, Zhou J-W, Lin S-H et al (2015) Characteristics and Causes of Groundwater Pollution after Hongshan-Zhaili Mine Closure in Zibo. Saf Environ Eng 22:23–28 (in Chinese)
34. Zhou R-M (2018) Excavation characteristics of Yudong coal mine, Kaili City, Guizhou Province.Inner Mongolia Coal Economy:145–146(in Chinese)
35. Zhou X, Ye Y-H (2014) Improvement and application of Schukalev groundwater hydrochemical classification method: taking groundwaters in Jinjiang city, Fujian Province as an Example. Resour Surv Environ 35:299–304 (in Chinese)

Figures

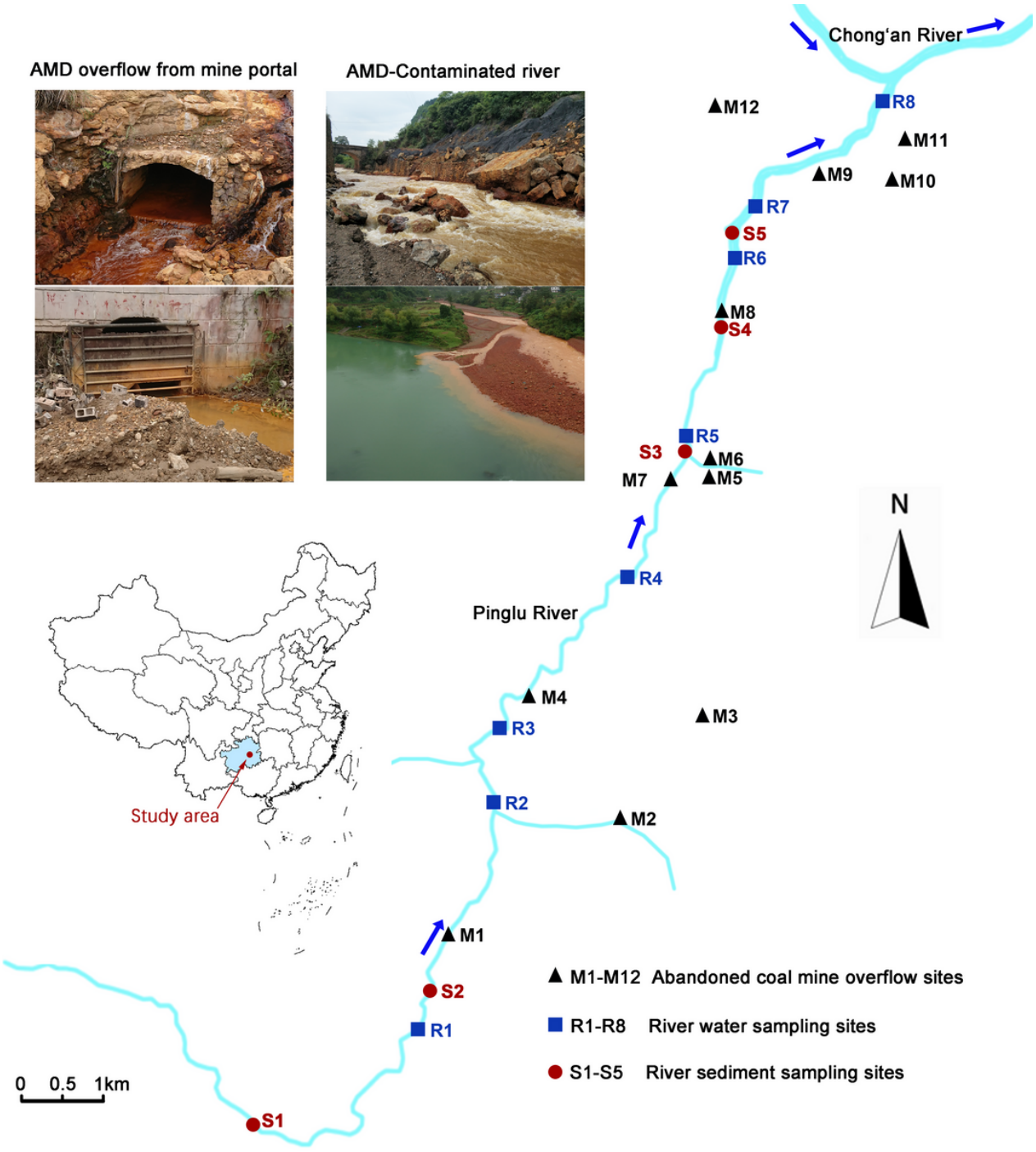

Figure 1

Study area and sampling sites

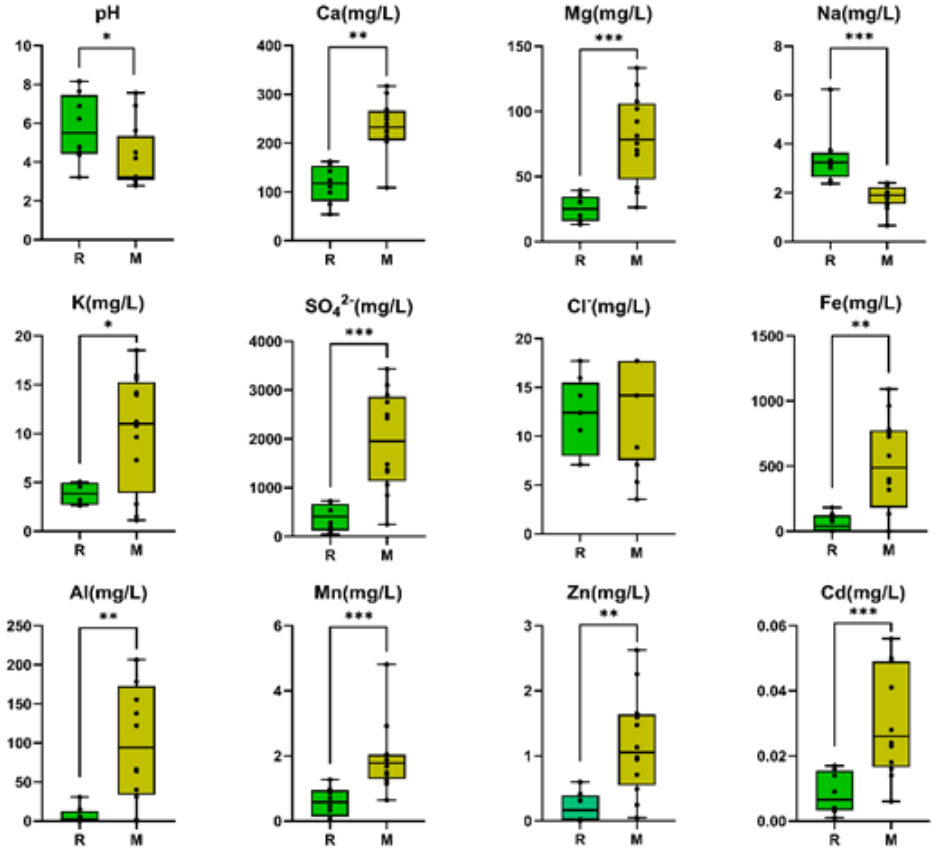

Figure 2

Box plots indicate the distribution and significant differences of physicochemical parameters between the two groups of water samples. Group R represents water samples collected from Pinglu River, and Group M represents samples collected from abandoned coal mine drainage

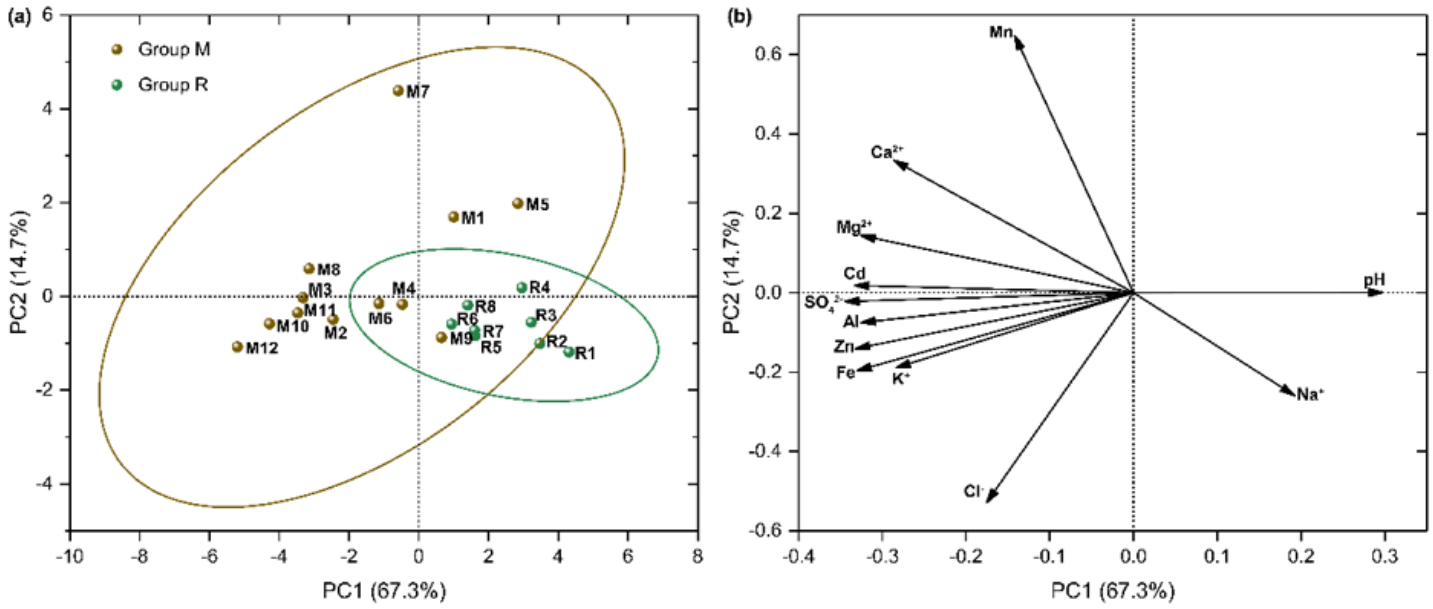

Figure 3

Principal component analysis (PCA) of physicochemical parameters water sample. (a) Similarity and difference of physicochemical indexes of water samples, color green represent river water samples and brown represents abandoned coal mine drainage samples (b) Explanation degree of each physicochemical index on the distribution of samples

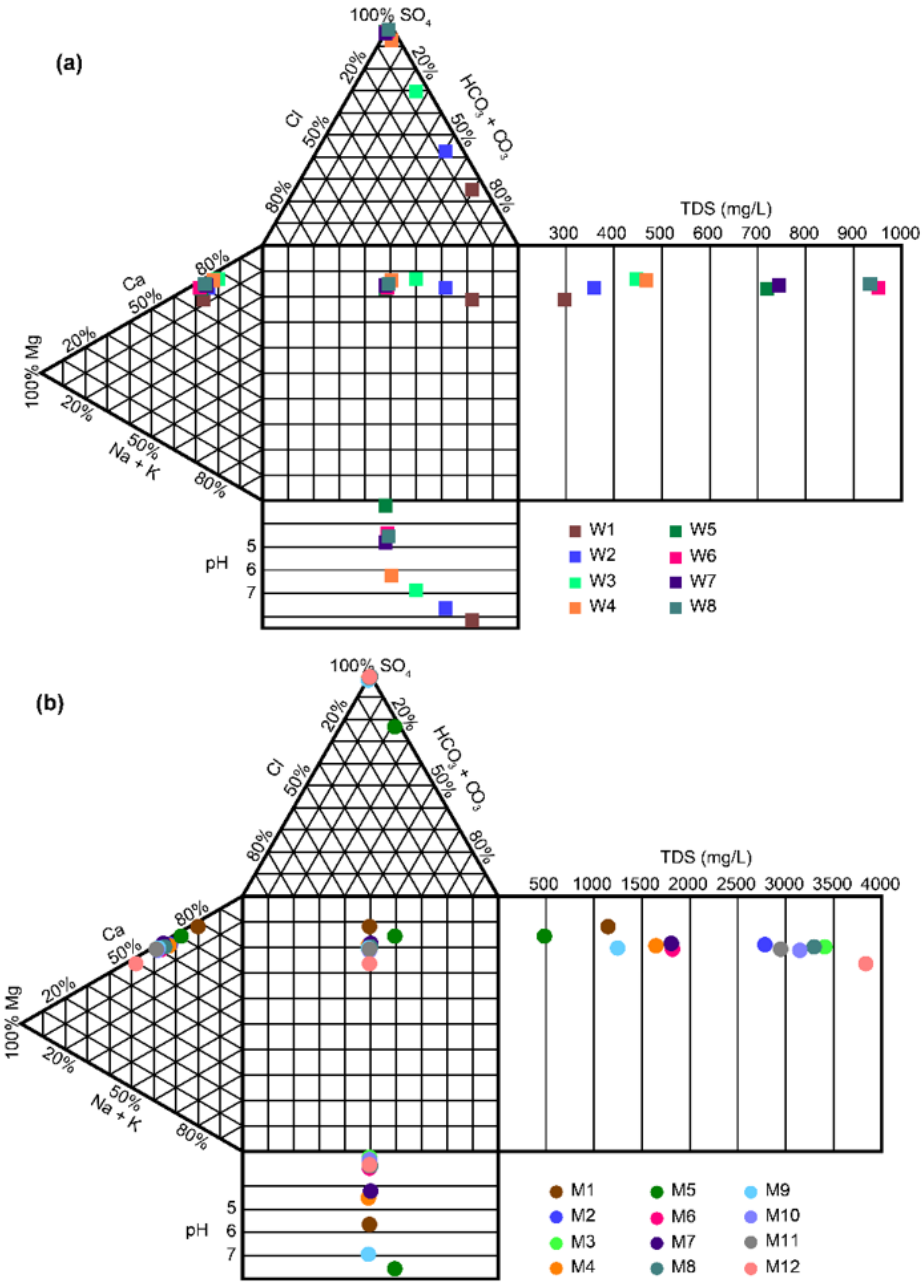

Figure 4

Hydrochemical characteristics of water samples (a) Abandoned coal mines water samples (b) River water samples

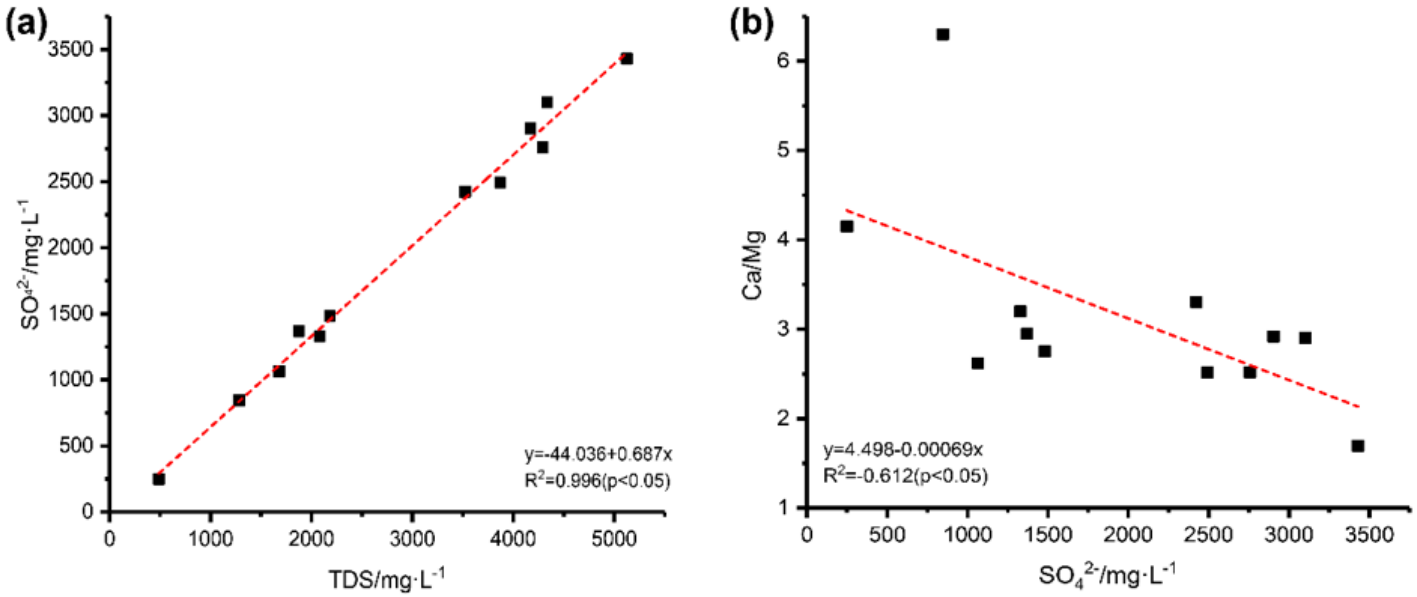

Figure 5

(a) TDS vs. SO_4^{2-} for abandoned coal mine drainage (b) Ca/Mg vs. SO_4^{2-} for abandoned coal mine drainage

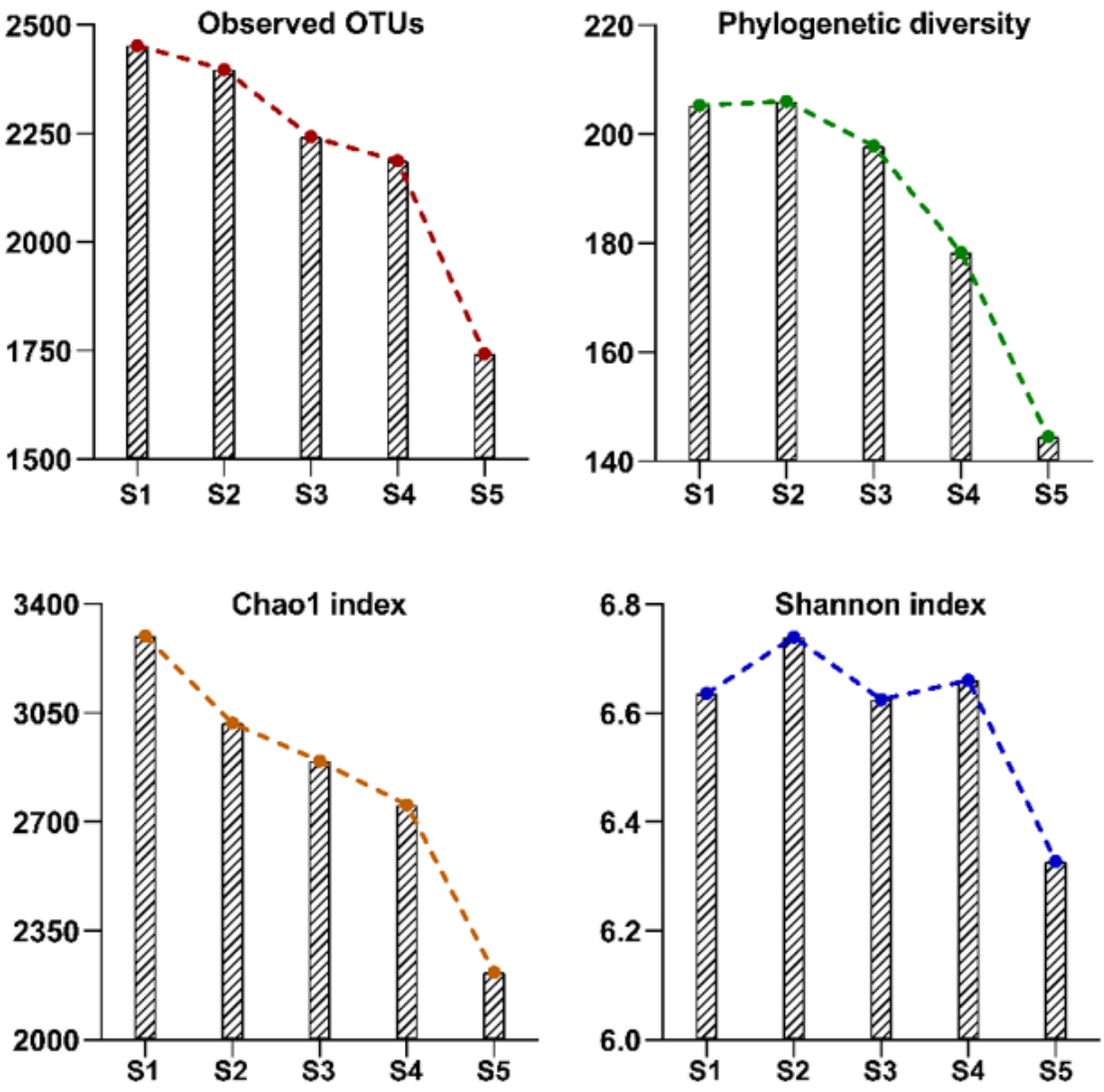

Figure 6

Variation of microbial Alpha indices along the river sediment

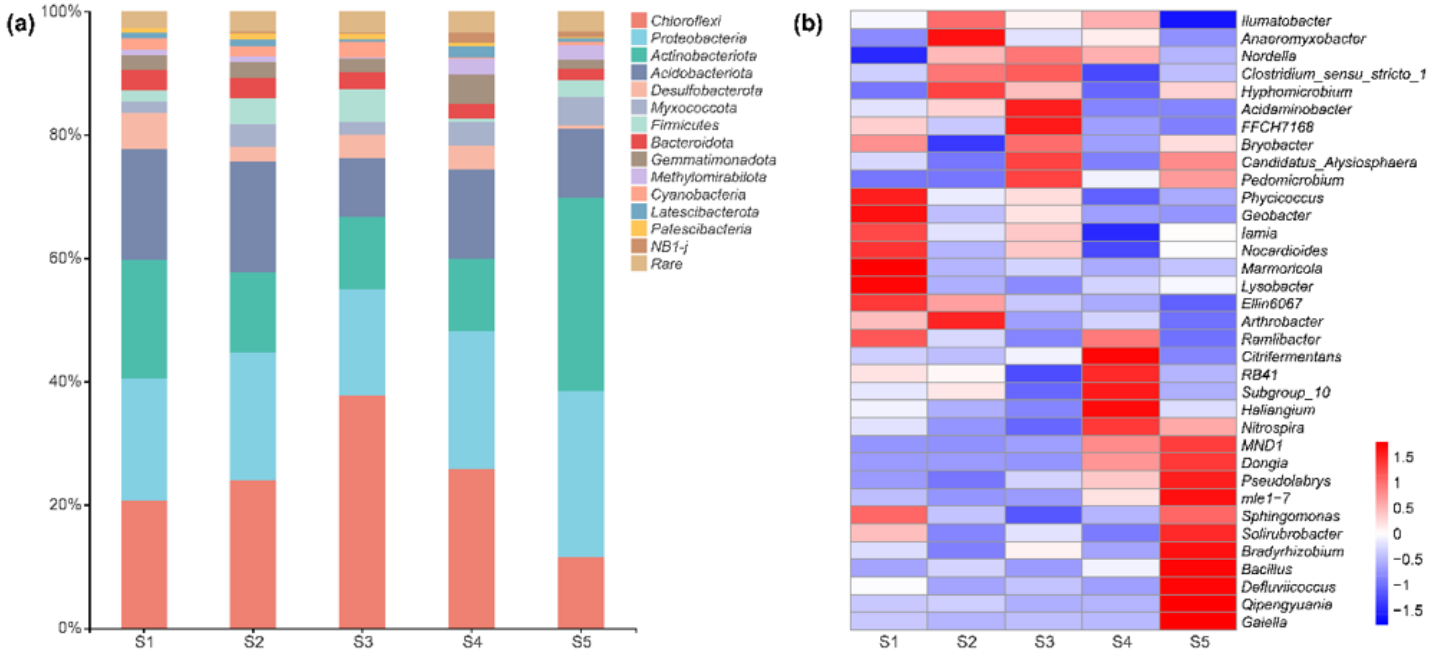

Figure 7

(a) Distribution of the top 15 most abundant phyla in sediment samples (b) Heatmap showing the clustering distribution of the top 35 dominant genera in samples

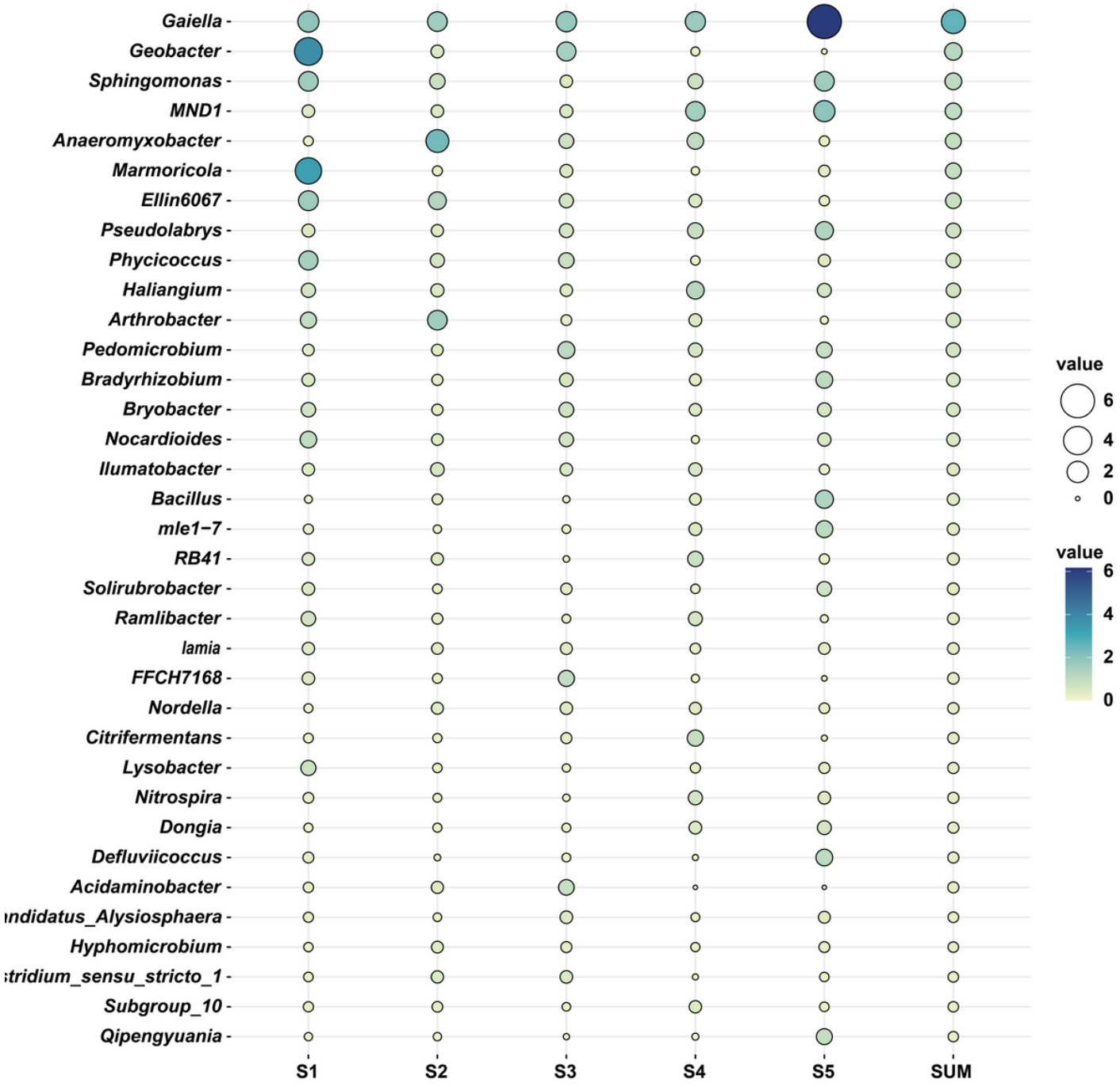

Figure 8

Distribution of the top 35 most abundant bacterial groups in sediment samples at genus level

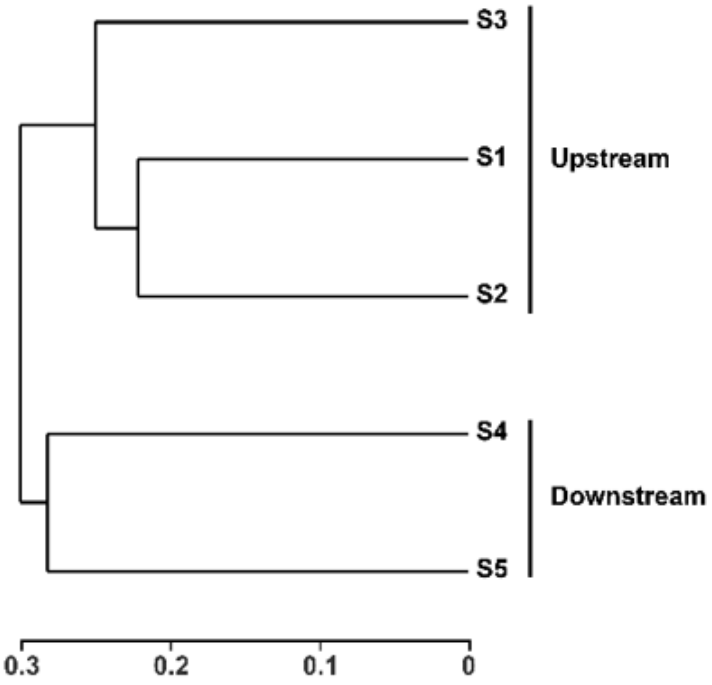

Figure 9

UPGMA tree showing clusters of microbial communities based on Bray-Curtis method with 100% support at all nodes

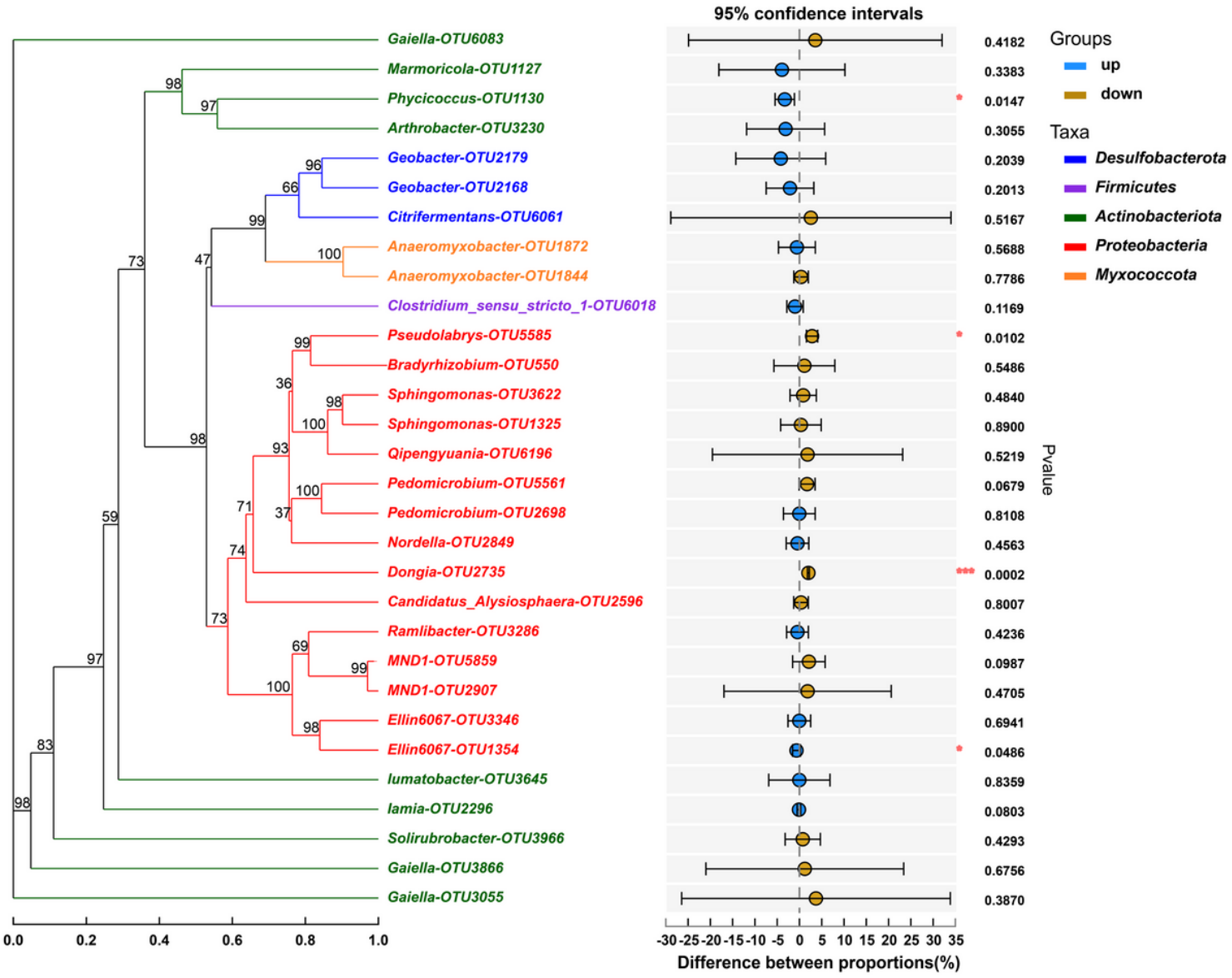

Figure 10

Phylogenetic tree of the top 30 OTUs in river sediment. The color of each OTU represents the assignment at phylum level. Statistical difference of the top 30 OTUs between upstream and downstream samples based on Welch's t-test were shown in the right

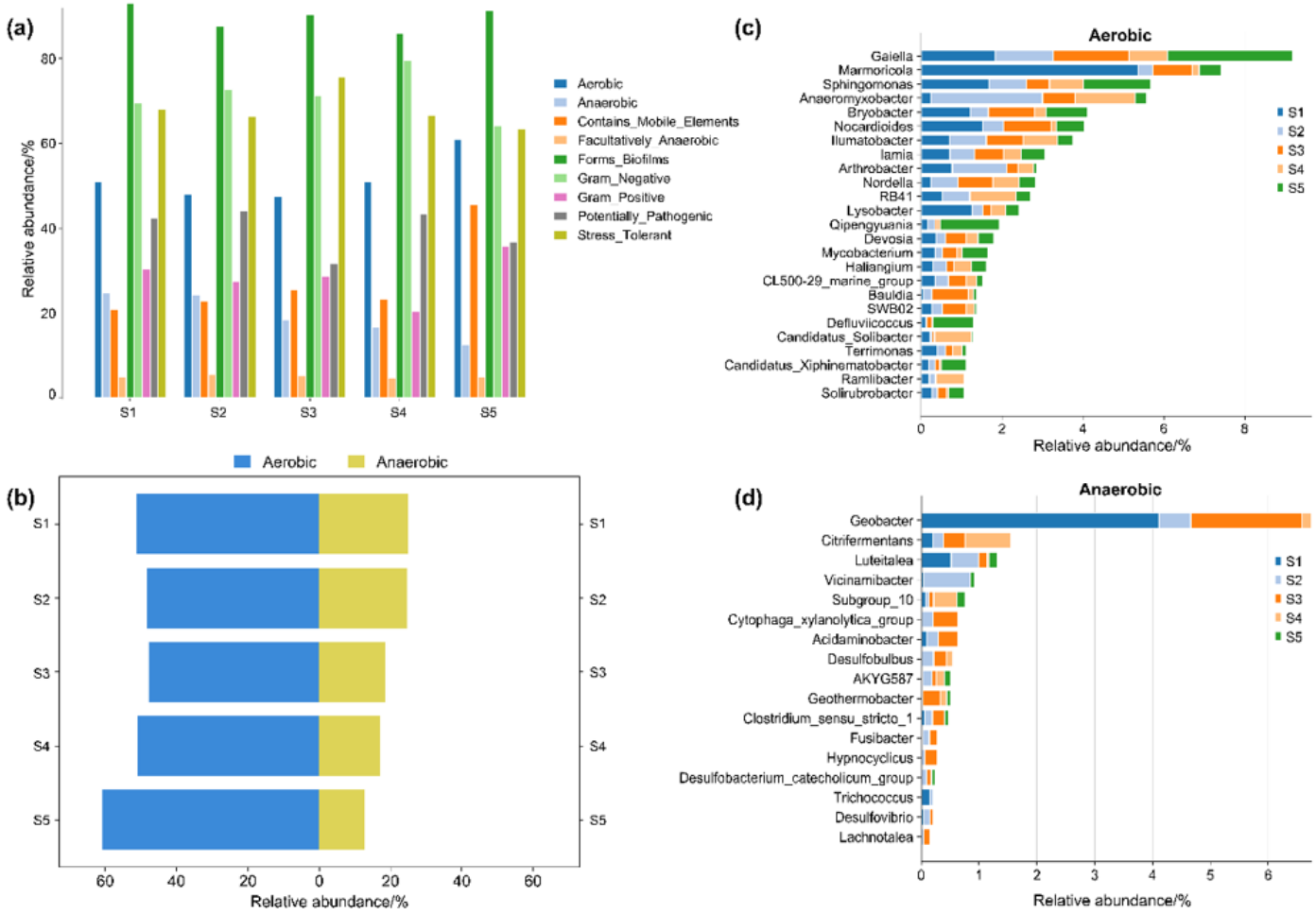

Figure 11

Phenotypic prediction of microbial communities in river sediments (a) Statistics of predicted river sediment phenotypes (b) Relative abundance of anaerobic and aerobic microorganisms in river sediments (c) Major contributing genera of aerobic microbial communities (d) Major contributing genera of anaerobic microbial communities

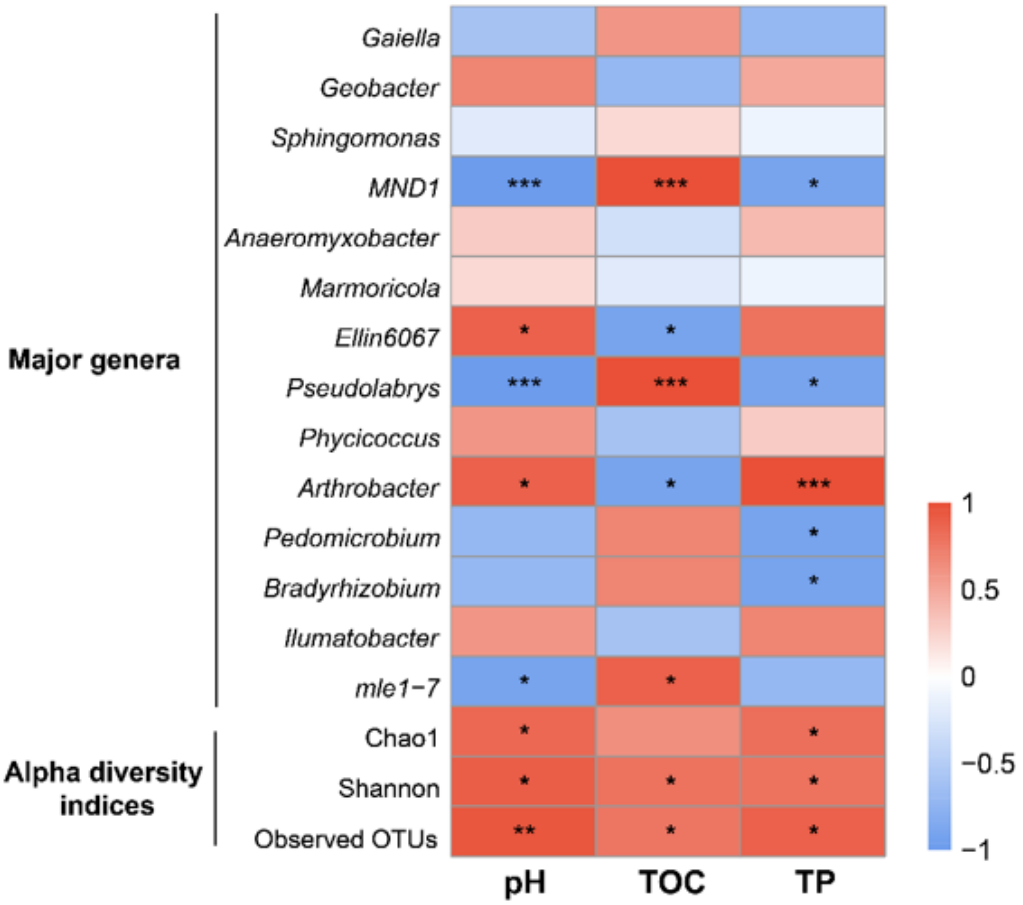

Figure 12

Correlation between the major bacterial genera, microbial diversity indices and pH, TOC and TP